

Nuclear structure study of $^{22,24}\text{Ne}$ and ^{24}Mg nuclei

Fouad A. Majeed, and Sarah M. Obaid

*Department of Physics, College of Education for Pure Sciences,
University of Babylon, Babylon, Iraq.*

*Department of Physics, College of Education for Pure Science (Ibn-Alhatham),
University of Baghdad, Baghdad, Iraq.*

Received 1 September 2018; accepted 9 October 2018

Shell model calculations based on large basis has been conducted to study the nuclear structure of ^{20}Ne , ^{22}Ne and ^{24}Mg nuclei. The energy levels, inelastic electron scattering form factors and transition probabilities are discussed by considering the contribution of configurations with high-energy beyond the model space of sd-shell model space which is denoted as the core polarization effects. The Core polarization is considered by taking the excitations of nucleus from the $1s$ and $1p$ core orbits and also from the valence $2s$ $1d$ shell orbits into higher shells with $4\hbar\omega$. The effective interactions $USDA$ and $USDB$ are employed with sd shell model space to perform the calculation and the core polarization are calculated with $MSDI$ as residual interaction. The calculated energy level schemes, form factors and transition probabilities were compared with the corresponding experimental data. The effect of core polarization is found very important for the calculation of $B(C2)$, $B(C4)$ and form factors, and gives excellent results in comparison with the experimental data without including any adjustable parameters.

Keywords: Nuclear structure; electron scattering form factors; core polarization effects.

PACS: 25.30.Dh; 21.60.Cs; 27.30.+t

1. Introduction

The nuclear shell model proved to be very successful tool to investigate the nuclear structure: by choosing an adequate residual effective interaction, the shell model able to account for various observables accurately and systematically. The nuclear structure study progressed by developing the nuclear shell model [1]. Although the shell model is basically simple, it explains many nuclear properties such as spin, magnetic moment, and nuclear spectra. The shell model is composed of two fundamental kinds of models which are related to the basis of the shell model: the models of the mean-field and they configuration mixing models [2]. The sd -shell is an interesting region for shell model calculations which can be investigated by elastic magnetic electron scattering, where the nucleus is considered as an inert ^{16}O and the full $1d_{5/2}$, $2s_{1/2}$, $1d_{3/2}$ space is used for the valance nucleons. Excitation to the higher shell are ignored in the model. Calculations based on this model may not be able to reproduce the experimental observations or to agree with the experimental form factors. Effective charges are adopted in many previous studies in which the effective g-factors were implied. The (q)-dependence of form factors on the momentum transfer resulting from configuration mixing is very different for a different major shell, and cannot in general be considered as a q independent scaling [3]. The shell model electron scattering form factors needs to be modified by including higher configurations, called core polarization effect. These effects are considered as a supplement to the usual shell-model treatments, which gives more practical efforts to account for the Coulomb excitations collectivity. A model based on microscopic approach has been used to account for CP effects between states of single particle with LS closed shell [4].

Radhi *et al.* [5–8] have argued previously that the CP effects are essential to be taken into consideration for nuclei lies in the p -shell and sd -shell to improve the calculations of the form factors. The single quadrupole transitions Coulomb form factors for electron scattering in the p -shell ^{10}B nucleus have been investigated by F. A. Majeed [9], in which $2\hbar\omega$ excitations were considered by prompting nucleons from the core orbits to higher orbits to account for CP effects. The high energy configuration effect were considered by means of core polarization effect have been investigated by Majeed *et al.* [10] on the $C2$ and $C4$ form factors of some selected nuclei lies in the fp -shell region. The core polarization were calculated by employing harmonic oscillator (HO) and Skyrme-Hartree Fock (Skx) as residual interactions. Majeed *et al.* [11] investigated the effect of the configuration of high energy for the positive and negative parity states form factors for longitudinal and transverse cases.

The goal of the current study is to investigate the nuclear structure of ^{20}Ne , ^{22}Ne and ^{24}Mg nuclei. In particular, energy levels, inelastic electron scattering form factors and transition probabilities using shell model codes CP and NushellX@MSU for windows [12]. The study of $C2$ and $C4$ for this nuclei including configurations of high-energies by utilizing the first-order perturbation theory to account for the CP effects. The zeroth contribution for the single-particle wave functions are used and the effect of CP , is taken into consideration by perturbation theory of first order with the residual interaction which is the modified surface delta interaction ($MSDI$) [13]. The potential of harmonic-oscillator (HO) with the size parameter b is taken to account for the root-mean-square (rms) charge radii of the studied nuclei.

The effect of CP on the form factors is derived from a

microscopic theory that allows the basis function of the shell and the configurations with higher-energy to be combined as perturbations of first order. The electron scattering operator T_Λ , written in terms of the reduced matrix elements which consists of the residual interaction V_{res} as the sum of the product of the density matrix of one-body (DMOB) elements $\chi_{\Gamma_f \Gamma_i}^\Lambda(\alpha, \beta)$ times the matrix element of single particle, and is given by,

$$\begin{aligned} \langle O_f ||| T_\Lambda ||| O_i \rangle &= \langle O_f ||| T_\Lambda ||| O_i \rangle_{\text{ms}} \\ &+ \langle O_f ||| \delta T_\Lambda ||| O_i \rangle_{\text{CP}}, \end{aligned} \quad (1)$$

where $|O_i\rangle$ and $|O_f\rangle$ are the model space states. The quantum numbers are denoted by Greek symbols in space and isospace coordinates, *i.e.* $O_i \equiv J_i T_i$, $O_f \equiv J_f T_f$ and $\Lambda = J T$.

The matrix of the model space (ms) consists of the sum of the product of the matrix element of the density matrix of one-body (DMOB) $\chi_{O_f O_i}^\Lambda(\alpha, \beta)$ times the matrix element of the single-particle as follows [14],

$$\langle O_f ||| T_\Lambda ||| O_i \rangle_{\text{ms}} = \sum_{\alpha, \beta} \chi_{O_f O_i}^\Lambda(\alpha, \beta) \langle \alpha ||| T_\Lambda ||| \beta \rangle, \quad (2)$$

with the single-particle states α and β are to account for the model space where the isospin is included.

The matrix element of the configurations with higher energy (CP) is similarly written as

$$\langle O_f ||| \delta T_\Lambda ||| O_i \rangle_{\text{CP}} = \sum_{\alpha, \beta} \chi_{O_f O_i}^\Lambda(\alpha, \beta) \langle \alpha ||| \delta T_\Lambda ||| \beta \rangle, \quad (3)$$

$$\begin{aligned} \langle \alpha ||| \delta T_\Lambda ||| \beta \rangle &= \langle \alpha ||| T_\Lambda \frac{Q}{E_i - H_0} V_{\text{res}} ||| \beta \rangle \\ &+ \langle \alpha ||| V_{\text{res}} \frac{Q}{E_f - H_0} T_\Lambda ||| \beta \rangle. \end{aligned} \quad (4)$$

where Q represent the projection operator, which projects onto the model space. The MSDI [13] is adopted as the residual interaction V_{res} and E_i and E_f are the energies of the initial and final states, respectively.

The MSDI effective interaction that was adopted for the calculation of the CP effects is a very adequate choice due to its adjustable parameters that allows us to reliably consider the CP effects with respect to the model space. The MSDI can be written as [13]

$$\begin{aligned} \langle j_1 j_2 | V_{(1,2)}^{\text{MSDI}} | j_3 j_4 \rangle_{JT} &= -A_T \frac{(2j_1 + 1)(2j_2 + 1)}{2(2J + 1)(1 + \delta_{12})} \\ &\times \left\{ \langle j_2 - \frac{1}{2} j_1 \frac{1}{2} | J0 \rangle^2 [1 - (-1)^{l_1 + l_2 + J + T}] + \langle j_2 \frac{1}{2} j_1 \frac{1}{2} | J1 \rangle^2 [1 - (-1)^T] \right\} \\ &+ \left[2T(T + 1) - 3 \right] + B + C \end{aligned} \quad (5)$$

where $\langle j_2 - (1/2)j_1(1/2) | J0 \rangle$, $\langle j_2(1/2)j_1(1/2) | J1 \rangle$ are Clebsch-Gordan coefficients [15], T is the nuclear isospin, B and C are parameters obtained from the fitting to the experimental data for various mass region. The parameters A_T with T taken as 0 or 1, B and C are approximated as [13]

$$A_0 \approx A_1 \approx B = \frac{25}{A} \quad \text{and} \quad C \approx 0, \quad (6)$$

where A is the mass number.

The CP terms are written as [13]

$$\begin{aligned} \langle \alpha ||| \delta T_\Lambda ||| \beta \rangle &= \sum_{\alpha_1, \alpha_2, \Gamma} \frac{(-1)^{\beta + \alpha_2 + \Gamma}}{e_\beta - e_\alpha - e_{\alpha_1} + e_{\alpha_2}} (2\Gamma + 1) \left\{ \begin{array}{ccc} \alpha & \beta & \Lambda \\ \alpha_2 & \alpha_1 & \Gamma \end{array} \right\} \sqrt{(1 + \delta_{\alpha_1 \alpha})(1 + \delta_{\alpha_2 \beta})} \\ &\times \langle \alpha \alpha_1 | V_{\text{res}} | \beta \alpha_2 \rangle \langle \alpha_2 ||| T_\Lambda ||| \alpha_1 \rangle + \text{terms with } \alpha_1 \text{ and } \alpha_2 \text{ exchanged with an overall minus sign} \end{aligned} \quad (7)$$

where α_1 and α_2 indices which runs over particles states and e is the energy for single-particle states. The CP terms are determined from the intermediate states up to the $2p1f$ -shells. The matrix element of the single-particle is reduced in both spin and isospin is expressed in terms of the matrix element of the single reduced in spin only [13].

$$\langle \alpha_2 ||| T_\Lambda ||| \alpha_1 \rangle = \sqrt{\frac{2T + 1}{2}} \sum_{t_z} I_T(t_z) \langle \alpha_2 || T_\Lambda || \alpha_1 \rangle \quad (8)$$

with

$$I_T(t_z) = \begin{cases} 1, & \text{for } T = 0, \\ (-1)^{1/2-t_z}, & \text{for } T = 1, \end{cases}$$

where $t_z = -1/2$ for neutrons and $1/2$ for protons. The matrix element of the single-particle Coulomb operator is expressed as [14]

$$\begin{aligned} & \langle \alpha_2 || T_J || \alpha_1 \rangle \\ &= \int_0^\infty dr r^2 j_J(qr) \langle \alpha_2 || Y_J || \alpha_1 \rangle R_{n_1 \ell_1} R_{n_2 \ell_2} \end{aligned} \quad (9)$$

where $j_J(qr)$ is the Bessel function in spherical coordinates and $R_{n\ell}(r)$ is the radial wavefunction for the single particle.

The form factors for electron scattering involves the momentum transfer q and angular momentum J , between the initial and final nuclear shell model states of spin $J_{i,f}$ and isospin $T_{i,f}$ [3] is [3]

$$\begin{aligned} |F_J(q)|^2 &= \frac{4\pi}{Z^2(2J_i + 1)} \left| \sum_{T=0,1} \begin{pmatrix} T_f & T & T_i \\ -T_z & 0 & T_z \end{pmatrix} \right|^2 \\ &\times |\langle \alpha_2 || T_\Lambda || \alpha_1 \rangle|^2 |F_{c.m}(q)|^2 |F_{f.s}(q)|^2 \end{aligned} \quad (10)$$

where T_z is the final isospin states projected along z-axis and is evaluated by the relation $T_z = (Z - N)/2$. The form factor for the finite size of the nucleon (f.s) is $F_{f.s}(q) = \exp(-0.43q^2/4)$ and $F_{c.m}(q) = \exp(q^2b^2/4A)$ represent the translational invariance lack in the shell model. A is the mass number and b is the size parameter for harmonic oscillator.

The strength of the electric transition is [13]

$$B(CJ, k) = \frac{Z^2}{4\pi} \left[\frac{(2J+1)!!}{k^J} \right]^2 F_J^2(k) \quad (11)$$

where $k = E_x/\hbar c$.

The Tassie model (TM) used for the core polarization in NushellX@MSU is a modelling of more elasticity and modification that allows a non-uniform mass and charge density distribution. The CP charge density in TM model depends on the ground state charge density of the nucleus. The ground state charge density is expressed in terms of the two-body charge density for all occupied shells including the core. Based on the collective modes of the nuclei, the Tassie shape core polarization transition density is given by [16].

$$\rho_{Jt_z}^{\text{core}}(i, f, r) = N \frac{1}{2} (1 + \tau_z) r^{J-1} \frac{d\rho_0(i, f, r)}{dr} \quad (12)$$

where N is a proportionality constant and ρ_0 is the ground state two-body charge density distribution, which is given

$$\rho_0 = \langle \psi | \hat{\rho}_{eff}^{(2)}(\vec{r}) | \psi \rangle = \sum_{i < j} \langle ij | \hat{\rho}_{eff}^{(2)}(\vec{r}) | ij \rangle - |ji \rangle \quad (13)$$

where

$$\hat{\rho}_{\text{eff}}^{(2)}(\vec{r}) = \frac{1}{2(A-1)} f(r_{ij}) \sum_{i \neq j} \{ \delta(\vec{r} - \vec{r}_i) + \delta(\vec{r} - \vec{r}_j) \} f(r_{ij})$$

i and j are all the required quantum numbers, *i.e.* $i \equiv n_i, \ell_i, j_i, m_i, t_i, m_{t_i}$ and $j \equiv n_j, \ell_j, j_j, m_j, t_j, m_{t_j}$ where the functions $f(r_{ij})$ are the two body short range correlation (SRC). In this work, a simple model form of short range correlation has been adopted, *i.e.*

$$f(r_{ij}) = 1 - \exp[-\beta(r_{ij} - r_c)^2]$$

where r_c is the radius of a suitable hard-core and β is a correlation parameter. The Coulomb form factor for this model becomes:-

$$\begin{aligned} F_J^L(q) &= \sqrt{\frac{4\pi}{2J_i + 1}} \frac{1}{Z} \left\{ \int_0^\infty r^2 j_J(qr) \rho_J^{ms}(i, f, r) dr \right. \\ &+ N \int_0^\infty dr r^2 j_J(qr) r^{J-1} \frac{d\rho_0(i, f, r)}{dr} \left. \right\} F_{c.m}(q) F_{f.c}(q) \end{aligned} \quad (14)$$

The radial integral

$$\int_0^\infty dr r^{J+1} j_J(qr) \frac{d\rho_0(i, f, r)}{dr}$$

can be written as:-

$$\begin{aligned} & \int_0^\infty \frac{d}{dr} \{ r^{J+1} j_J(qr) \rho_0(i, f, r) \} dr \\ & - \int_0^\infty dr (J+1) r^J j_J(qr) \rho_0(i, f, r) \\ & - \int_0^\infty dr r^{J+1} \frac{d}{dr} j_J(qr) \rho_0(i, f, r) \end{aligned} \quad (15)$$

where the first term gives zero contribution, the second and the third term can be combined together as

$$-q \int_0^\infty dr r^{J+1} \rho_0(i, f, r) \left[\frac{d}{d(qr)} + \frac{J+1}{qr} \right] j_J(qr) \quad (16)$$

from the recursion of the spherical Bessel function:

$$\left[\frac{d}{d(qr)} + \frac{J+1}{qr} \right] j_J(qr) = j_{J-1}(qr) \quad (17)$$

$$\begin{aligned} & \therefore \int_0^\infty dr r^{J+1} j_J(qr) \frac{d\rho_0(i, f, r)}{dr} \\ & = -q \int_0^\infty dr r^{J+1} j_{J-1}(qr) \rho_0(i, f, r) \end{aligned}$$

Therefore, the form factor of Eq. (number) takes the form:

$$F_J^L(q) = \left(\frac{4\pi}{2J_i + 1} \right)^{1/2} \frac{1}{Z} \left\{ \int_0^\infty r^2 j_J(qr) \rho_{Jt_z}^{ms} dr - Nq \int_0^\infty dr r^{J+1} \rho_0 j_{J-1}(qr) \right\} \times F_{cm}(q) F_{fs}(q) \quad (18)$$

The proportionality constant N can be determined from the form factor evaluated at $q = k$, *i.e.* substituting $q = k$ in the equation above we obtained

$$N = \frac{\int_0^\infty dr r^2 j_J(kr) \rho_{Jt_z}^{ms}(i, f, r) - F_J^L(k) Z \sqrt{\frac{2J_i+1}{4\pi}}}{\int_0^\infty dr r^{J+1} \rho_0(i, f, r) j_{J-1}(kr)} \quad (19)$$

2. Results and Discussion

2.1. The excitation energies

The core is taken at ^{16}O for all nuclei under the study with 4, 6 and 8 particles outside the core for ^{20}Ne , ^{22}Ne and ^{24}Mg respectively. Figure 1 displays our theoretical work in comparison to the experimental data [18] for ^{20}Ne nucleus. Our calculations predicts the values 2^+ at 1.696 MeV and 1.747 MeV, by employing the effective interactions *usda* and *usdb*, respectively. The difference between 2^+ is found to be 62 keV and 113 keV in comparison with the corresponding experimental data using *usda* and *usdb*, respectively. The 1^+ has been confirmed by our theoretical calculations which is not confirmed experimentally using both effective interactions. The theoretical prediction compared to the the corresponding experimental data of the energy levels for positive parity states of ^{22}Ne nucleus is shown in Fig. 2. Our calculations predicts the values 2^+ at 1.310 MeV and 1.363 MeV, by utilizing the effective interactions *usda* and *usdb*, respectively. The difference between 2^+ is found to be 35 KeV and 88 keV in comparison with the corresponding experimental data using *usda* and *usdb*, respectively. Many unconfirmed experimental energy levels for this nucleus have been con-

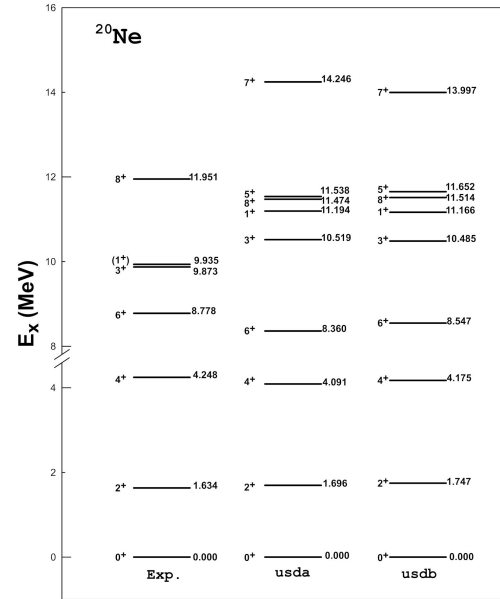


FIGURE 1. Calculations of the excitation energies compared to the corresponding experimental data [18] using *usda* and *usdb* effective interactions for ^{20}Ne nucleus.

firmed. Figure 3 shows the theoretical energy spectra for ^{24}Mg nucleus in comparison with the experimental data [18]. The predicted values for 2^+ levels is found at 1.491 MeV and 1.502 MeV using *usda* and *usdb* effective interactions, respectively. The absolute difference for the 2^+ level and the corresponding experimental data is 122 keV and 133 keV using *usda* and *usdb* effective interactions, respectively. All the energy levels ordering is predicted correctly for ^{24}Mg nucleus.

2.2. Electron scattering form factors

The *MSDI* residual effective interaction is employed to calculate the *CP* effects. The parameters of the *MSDI* residual effective interaction are A_T , B and C [13], where T is the isospin which takes the values 0 or 1. The *MSDI* parameters are estimated from $A_0 = A_1 = B = 25/A$ and $C = 0$, where A represent the mass number. In all the proceeding figures below “see Fig. 1 panel (a)”, the dashed curve

TABLE I. The estimated values of the reduced transition probabilities $B(C2 \uparrow)$ (in units of $e^2 fm^4$) and $B(C4 \uparrow)$ (in units of $e^2 fm^8 \times 10^3$) compared with the corresponding experimental data.

Nucleus	J_f^π	T_f	$E_x(\text{MeV})$	ms	ms+CP	Exp.
^{20}Ne	2_1^+	0	1.634	145.1	461.3	292.07 ± 37.72^a
	4_1^+	0	4.247	12.07	55.98	38 ± 8^b
^{22}Ne	2_1^+	0	1.275	166	248.7	229.8 ± 42^c
	4_1^+	0	3.357	4.42	9.02	—
^{24}Mg	2_1^+	0	1.369	119.5	390.7	428.9 ± 8.74^a
	2_2^+	0	4.238	12.17	25.47	22.37 ± 0.053^a
	4_2^+	0	6.011	11.75	23.98	43 ± 6^d

^aRef. [19], ^bRef. [20], ^cRef. [21], ^dRef. [22].

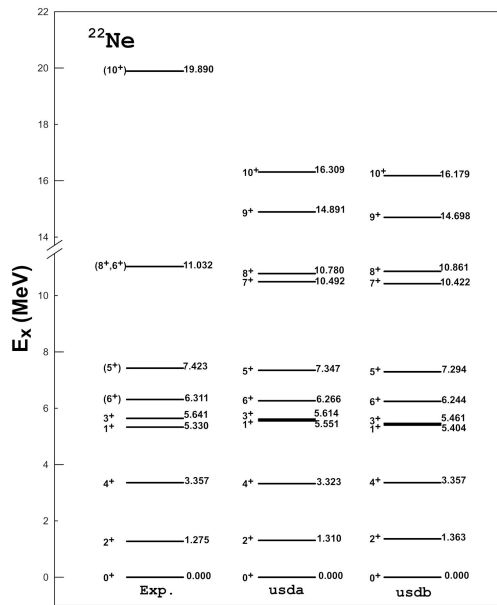


FIGURE 2. Calculations of the excitation energies compared to the corresponding experimental data [18] using *usda* and *usdb* effective interactions for ^{22}Ne nucleus.

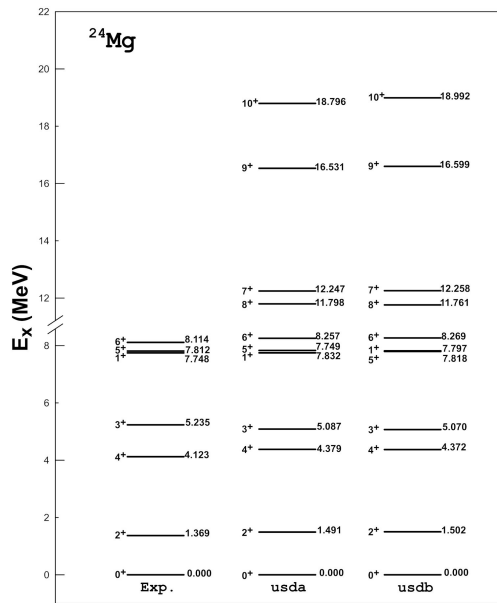


FIGURE 3. Calculations of the excitation energies compared to the corresponding experimental data [18] using *usda* and *usdb* effective interactions for ^{24}Mg nucleus.

gives the results obtained using the *sd* shell model calculations without *CP* effects. The dotted curve represents the contribution from the *CP* only. The blue solid curves represent the calculations including the core polarization contribution over the model space calculations (*sd* + *CP*) and the red solid line gives the results obtained for the Tassie model from NushellX with different set of proton e_π and e_ν effective charges.

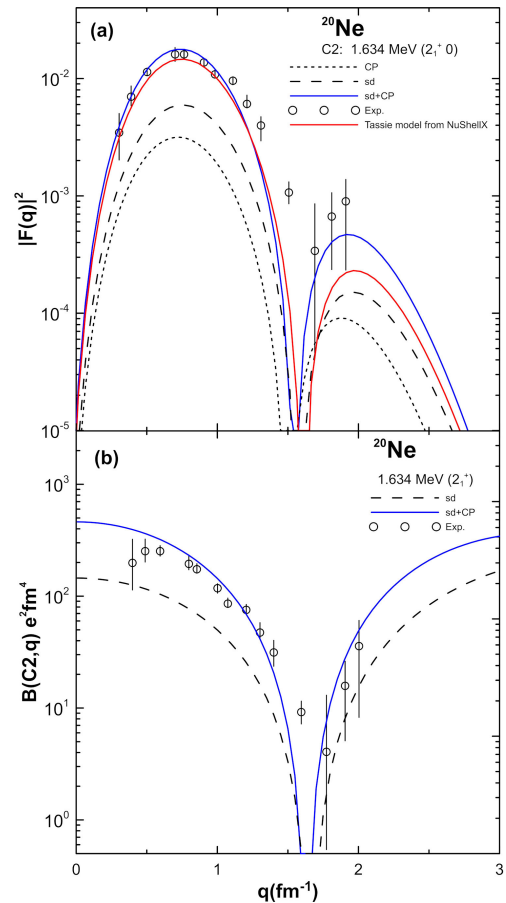


FIGURE 4. Panel (a) the longitudinal $C2$ form factor for 2^+_1 (1.634 MeV) in ^{20}Ne . The measured values are from Ref. [23] and panel (b) is the theoretical and experimental $B(C2, q)$ for the 1.634 MeV (2^+_1) state of ^{20}Ne .

2.2.1. ^{20}Ne Nucleus

1.634 MeV, $J_f^\pi T = 2^+_1 0$ state

Figure 4 panel (a) displayed the $C2$ form factor calculation for the state ($J_f^\pi T = 2^+_1 0$) at $E_x = 1.634$ MeV. The calculations of the *sd* shell model space only underestimates the experimental data, when the *CP* effects are considered, the calculation improved markedly, that made the form factor reproduce the experimental data over the entire range of the momentum transfer q . The predicted value of the $B(C2 \uparrow)$ for the *sd*-shell is $145.1 e^2 fm^4$ compared to the measured value $292.07 \pm 37.72 e^2 fm^4$ [19]. Including the *CP* effect in the calculations of the $B(C2 \uparrow)$ predicts the value to be $461.3 e^2 fm^4$. The Tassie model calculations agrees reasonably well with the first diffractions maxima and able to locate the experimental diffraction minima. The Tassie model underestimate the measured data in the second diffraction maxima. In general the $B(C2 \uparrow)$ reproduce the shape of the form factor and the theoretical calculation of the transition probability agrees reasonably well with the corresponding experimental probability as shown in Fig. 1 panel (b) for the state

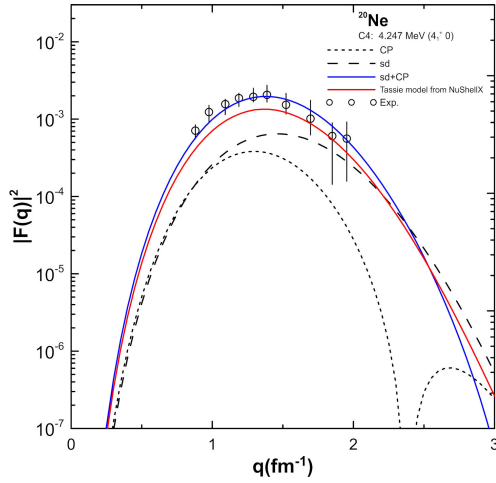


FIGURE 5. The longitudinal $C4$ form factor for 4_1^+ (4.247 MeV) in ^{20}Ne . The measured data from [23].

2_1^+ at 1.634 MeV. The inclusion of the CP effects is found to be very essential for both form factor and $B(C2 \uparrow)$ calculations.

4.247 MeV, $J_f^\pi T = 4_1^+ 0$ state

Figure 5 presents the $C4$ form factor calculation in which the sd -shell model predictions are lower than the experiment and considering the CP effects improves the form factor calculations that reproduced the experiment in detail all over the entire range of the momentum transfer q . The calculated $B(C2 \uparrow)$ value is $12.07 \times 10^3 e^2 fm^8$ excluding CP effects and $55.98 \times 10^3 e^2 fm^8$ including the CP effects along with the measured value $38 \pm 8 e^2 fm^8$ [20]. The Tassie model calculations underestimate the measured data in all momentum transfer dependence.

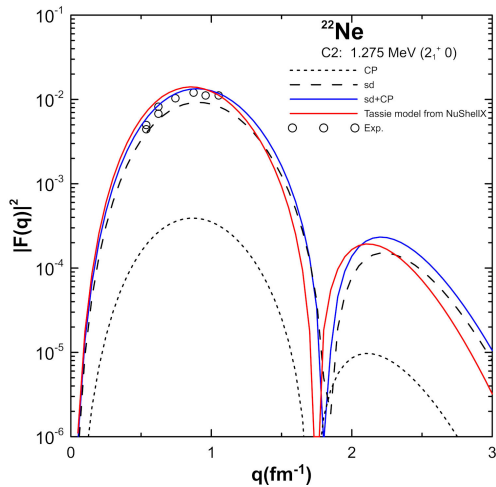


FIGURE 6. The longitudinal $C2$ form factor for 2_1^+ (1.275 MeV) in ^{22}Ne . The measured data from [24].

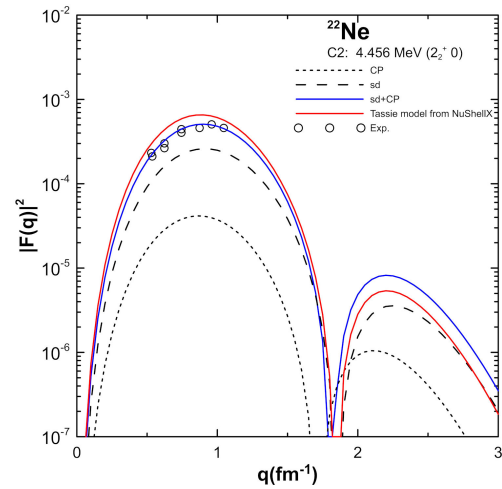


FIGURE 7. The longitudinal $C2$ form factor for 2_2^+ (4.456 MeV) in ^{22}Ne . The measured data from [24].

2.2.2. ^{22}Ne Nucleus

1.275 MeV, $J_f^\pi T = 2_1^+ 0$ state and 4.456 MeV, $J_f^\pi T = 2_2^+ 0$ state.

The form factor for the $C2$ transition for the states 2_1^+ and 2_2^+ calculations are displayed in Figs. 6 and 7, respectively. The sd -shell model calculations has a shortfall in describing the experimental form factors and the $(sd + CP)$ calculations are remarkably agreed with the measured values. The model space predicts the value $B(C2 \uparrow)$ to be $166 e^2 fm^4$ in comparison with the measured value $229.8 \pm 42 e^2 fm^4$. The calculated $B(C2 \uparrow)$ including the CP effects predicts the value of $248.7 e^2 fm^4$. The Tassie model overshoots the measured data for the $C2$ form factor.

3.357 MeV, $J_f^\pi T = 4_1^+ 0$ state

Figure 8 displays the $C4$ form factor of the longitudinal transition for the $J_f^\pi T = 4_1^+ 0$ state at $E_x = 3.357$ MeV of ^{22}Ne .

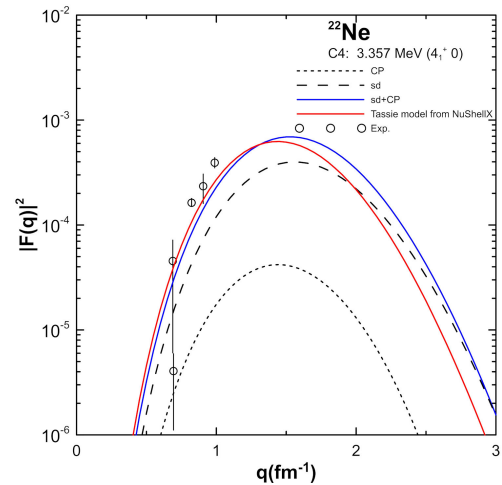


FIGURE 8. The longitudinal $C4$ form factor for 4_1^+ (3.357 MeV) in ^{22}Ne . The measured data from [24].

Theoretical model space predictions underestimate the measured values. The model space calculations along with CP effects taken into consideration improves the form factors calculations up to $q < 1.0\text{fm}^{-1}$. The predicted value of $B(C2 \uparrow)$ is $4.42 e^2\text{fm}^8 \times 10^3$ without the CP effects and $9.02 e^2\text{fm}^8 \times 10^3$ when the CP effects included. The Tassie model calculations with effective charges reproduce the measured data better than the model space calculations including the CP effects in the momentum transfer region up to $q < 1\text{fm}^{-1}$. The success of the Tassie model for this state might be attributed to the charge density that has a direct effect from the proton and neutron effective charges.

2.2.3. ^{24}Mg Nucleus

1.369 MeV, $J_f^\pi T = 2_1^+ 0$ state

The form factor for $C2$ transition state ($J_f^\pi = 2^+, T = 0$) at $E_x = 1.369$ MeV of the ^{24}Mg is displayed in Fig. 9 panel (a) where the model space calculations have a shortfall in describing the measured data. There is a remarkable enhancement in the calculations of the form factors for the first maxima and overshoots the data at the second maxima when

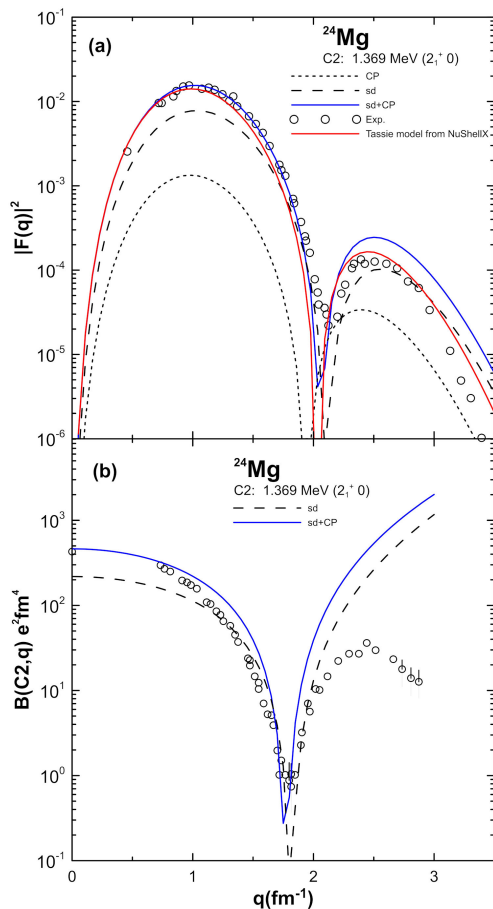


FIGURE 9. Panel (a) the longitudinal $C2$ form factor for $2_1^+ 0$ (1.369 MeV) state in ^{24}Mg . The measured values from [22] and panel (b) theoretical and experimental $B(C2, q)$ for the 1.369 MeV (2_1^+) state of ^{24}Mg .

the CP effects are included. The Tassie calculations reproduce the second maxima better than $sd + CP$ calculations and this might be attributed to the effective charge used for this state. The model space estimate the value of $B(C2 \uparrow)$ to be $119.5 e^2\text{fm}^4$, while the $sd + CP$ with $usda$ effective interaction is $390.7 e^2\text{fm}^4$ compared to the measured value $428.9 \pm 8.74 e^2\text{fm}^4$ [19]. The comparison of the calculated $B(C2, q)$ as function of the momentum transfer with the corresponding experimental data are shown in Fig. 9 panel (b). The model space calculations of $B(C2, q)$ underestimated the measured data in the momentum transfer region $0 \leq q \leq 1.2\text{fm}^{-1}$. The sd and $(sd + CP)$ calculations are both able to locate the diffraction minima accurately. The $B(C2, q)$ calculations start to deviate in the region $0 \leq q \leq 2.0\text{fm}^{-1}$ and the $(sd+CP)$ calculations improved markedly to agree reasonably well with the experimental data. The location of the diffraction minima of $B(C2, q)$ is located accurately for both sd and $sd + CP$ calculations. The calculated transition strength $B(C2 \uparrow)$ is $390.7 e^2\text{fm}^4$ agrees very well with the measured value

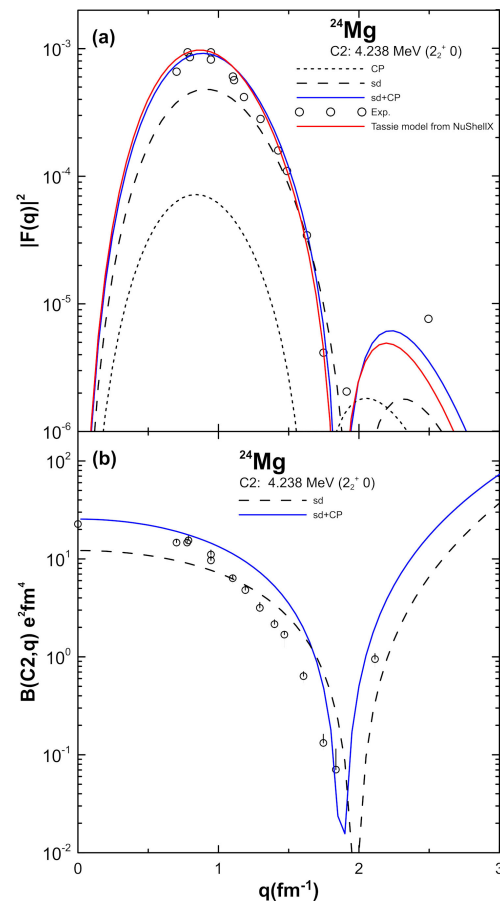


FIGURE 10. Panel (a) the longitudinal $C2$ form factor for $2_2^+ 0$ (4.238 MeV) in ^{24}Mg . The data are taken from [25] and panel (b) theoretical and experimental $B(C2, q)$ for the 4.238 MeV (2_2^+) state of ^{24}Mg .

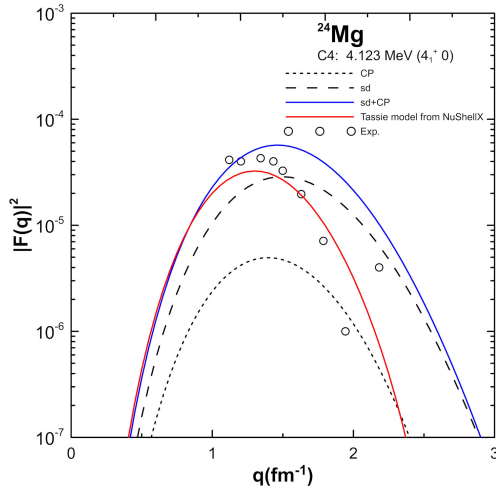


FIGURE 11. The longitudinal $C2$ form factor for 4_1^+0 (4.123 MeV) in ^{24}Mg . Measured values from [25].

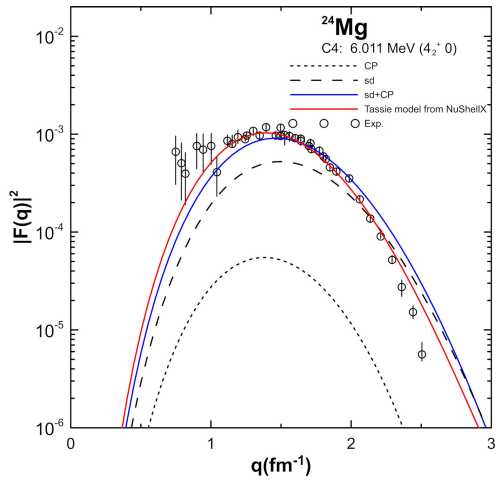


FIGURE 12. The longitudinal $C2$ form factor for 4_2^+0 (6.011 MeV) in ^{24}Mg . Measured values from [25].

$B(C2 \uparrow)$ is $428.9 \pm 8.74 e^2 fm^4$ which is obtained at the limit $q \rightarrow 0$. The Tassie model calculations of the $C2$ form factor for this state are in excellent agreement in all momentum transfer regions and are more closer to describe the second maxima at high momentum transfer.

4.238 MeV, $J_f^\pi T = 2_2^+0$ state

Figure 10 panel (a) presents the calculations of the 2_2^+0 (4.238 MeV) state. The calculations without the inclusion of CP effects have a shortfall in describing the measured data. The (sd + CP) calculations are in remarkably better agreement with the experimental data. CP effects enhance the form factor and reproduce the measured form factor in the first maxima. The model space calculations for $B(C2 \uparrow)$ gives $12.17 e^2 fm^4$ value in comparison with the measured

value of $22.37 \pm 0.053 e^2 fm^4$ [19] and including the CP effects predicts the value $25.47 e^2 fm^4$. The Tassie model calculations are very close to the model space calculations especially in the first maxima. The measured data in the high momentum transfer are very few, that we can not decide which one is in better agreement with the experiment. The calculation of the $B(C2 \uparrow)$ for the 2_2^+ state are shown by Fig. 10 panel (b) where the model space calculations underestimate the measured data, the $sd + CP$ calculations are able to reproduce the measured $B(C2 \uparrow)$ values for the momentum transfer region $q \geq 2.1 fm^{-1}$ and fail to reproduce that measured data $2.1 \leq q \leq 3.5 fm^{-1}$.

4.123 MeV, $J_f^\pi T = 4_1^+0$ state and 6.011 MeV, $J_f^\pi T = 4_2^+0$ state

The form factor for the transition $C4$ of the states (4.123 MeV, 6.011 MeV) 4_1^+ and 4_2^+ calculations are manifested in Figs. 11 and 12 respectively. The model space have a shortfall in reproducing the measured data and when the CP effects are considered, the calculations improved very well to be able to reproduce the measured data. The Tassie model with effective charges for proton and neutron is able to reproduce the data for both studied states. The calculated transition probability $B(C4 \uparrow)$ without include CP effect is $11.75 e^2 fm^4 \times 10^3$, compared with the measured value $43 \pm 6 e^2 fm^4 \times 10^3$ [22] and the predicted value with CP effects included is $23.98 e^2 fm^8 \times 10^3$.

3. Conclusion

The nuclear structure of ^{20}Ne , ^{22}Ne and ^{24}Mg nuclei have been studied by employing the shell model with $usda$ and $usdb$ effective interactions designed for the sd -shell region. The core polarization effects have been considered by a microscopic theory that allows the excitation to $4\hbar\omega$, without any adjustable parameters that were used previously when the core polarization effects is taken by the concept of the effective proton and neutron effective charges. The level excitation spectra, transition probabilities and inelastic electron scattering form factors have been addressed in the present study. The shell model prediction have a shortfall in describing the form factors and the CP effect must be taken into consideration to be able to reproduce the longitudinal $C2$ and $C4$ form factors. The Tassie model with proton and neutron effective charges is able to reproduce the $C2$ and $C4$ form factors for all the studied states of the nuclei under study.

Acknowledgments

Authors are grateful to Prof. R. A. Radhi for providing them with his core polarization code and for fruitful discussion and suggestions to improve the work.

1. R. R. Roy and B. P. Nigam, *Nuclear Physics Theory and Experiment*, John Willey and Sons Inc, (1967).
2. B. A. Brown, *Nucl. Phys. A* **704** (2002) 11-20.
3. T. W. Donnelly and I. Sick, *Rev. Mod. Phys.* **56** (1984) 461.
4. Y. Horikawa, T. Hoshino, and A. Arima, *Nucl. Phys. A* **278** (1977) 297-318.
5. R. A. Radhi, A. A. Abdullah, Z. A. Dakhil, and N. M. Adeeb, *Nucl. Phys. A* **696** (2001) 442-452.
6. R. A. Radhi, *Nuclear Physics A* **707** (2002) 56-64.
7. R. A. Radhi, *Eur. Phys. J. A.* **16** (2003) 381-385.
8. R. A. Radhi and A. Bouchebak, *Nucl. Phys. A* **716** (2003) 87-99.
9. Fouad A. Majeed, *Physica Scripta* **85** (2012) 065201.
10. Fouad A. Majeed and Fatima M. Hussain, *Rom. Journ. Phys.* **85** (2014) 065201.
11. F. A. Majeed and L. A. Najim, *Indian J. Phys* **89** (2015) 611-618.
12. B. A. Brown and W. D. M. Rae, *Nucl. Data Sheets* **120** (2014) 115-118.
13. P. J. Brussaard and P. W. M. Glaudemans, “*Shell-Model Applications in Nuclear Spectroscopy*” Amsterdam: North-Holland, (1977).
14. B. A. Brown, R. Radhi, and B. H. Wildenthal, *Phys. Rep.* **101** (1983) 313-358.
15. A. R. Edmonds, *Princeton university press* (2016).
16. L. J. Tassie, *Aust. J. Phys.* **9** (1956) 407-418.
17. T. de Forest Jr., J. D. Walecka, *Adv. Phys.* **15** (1966) 1-109.
18. J. Tuli, *Evaluated nuclear structure data file (ensdf)*. (Accessed March, 13, 2018).
19. P. M. Endt, *At. Data Nucl. Data Tables* **23** (1979) 547-585.
20. R. P. Singhal, H. S. Caplan, J. R. Moreira, and T. E. Drake, *Can. J. Phys* **51** (1973) 2125-2137.
21. B. Pritychenko, M. Birch, M. Horoi and B. Singh, *Nucl. data Sheets* **51** (2014) 112-114.
22. G. C. Li, M. R. Yearian, and I. Sick, *Phys. Rev. C* **9** (1974) 1861.
23. Y. Horikawa, Y. Torizuka, A. Nakada, S. Mitsunobu, Y. Kojima, and M. Kimura, *Phys. Lett. B*, **36** (1971) 9-11.
24. X. K. Maruyama *et al.*, *Phys. Rev. C* **19** 1624.
25. H. Zarek *et al.*, *Phys. Lett. B* **80** (1978) 26-29.